



Hairi Cipta<sup>1</sup>, Widyanto Dwi Nugroho<sup>2</sup>, Suyako Tazuru<sup>1</sup>, Junji Sugiyama<sup>1</sup>

<sup>1</sup>Research Institute for Sustainable Humanosphere, Kyoto University, Gokasho, Uji, Kyoto 611-0011, Japan

<sup>2</sup>Faculty of Forestry, Universitas Gadjah Mada, Jalan Agro No. 1 Bulaksumur, Yogyakarta 55281, Indonesia

## Introduction

### Keris

UNESCO recognised Keris as an intangible heritage from Indonesia. For keris sheath, usually using wood as the main material.

Limited information about the wood selection, especially about wood anatomical features.



### Wood identification

Wood identification is usually conducted by preparing thin section observed under optical microscope



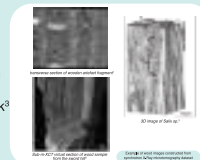
#### Disadvantages

- time consuming
- need experience & skill
- need much samples
- destructive

Not applicable for cultural wood

### Synchrotron X-Ray microtomography for identifying cultural wood

- Identification of wood taxa selected for archaeological artefact manufacture in Australia<sup>1</sup>
- Identification of wooden artefact from excavated grave<sup>2</sup>
- Identification of Korean wooden mask<sup>3</sup>

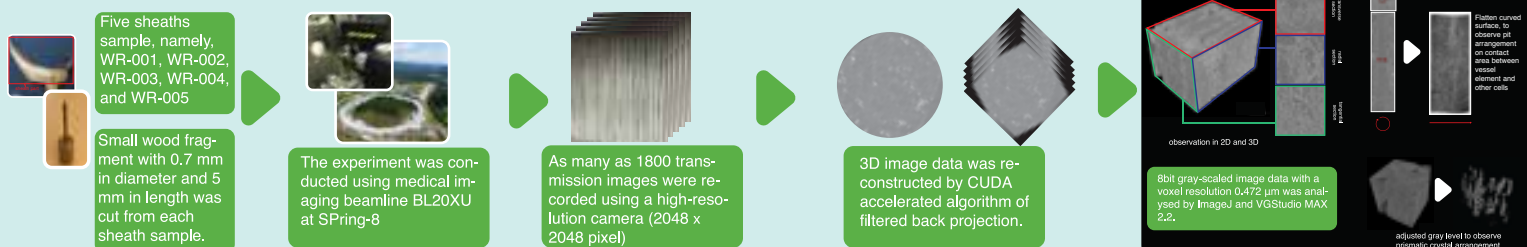


<sup>1</sup>Whitau et al., Journal of Archaeological Science: Reports 6 (2016) 536–546  
<sup>2</sup>Stebner & Milon, Journal of Archaeological Science 55 (2015) 188–196  
<sup>3</sup>Munro et al., Journal of Archaeological Science 37 (2010) 2842–2849

## Aim

Identify the species that is used as material of wooden keris sheath from Indonesia

## Materials and Method



## Results and Discussion

### Two-dimensional (2D) and Three-dimensional (3D) image of samples

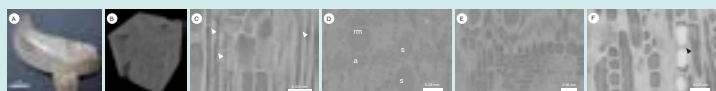


**Figure 1.** Observation of sample WR-001: photograph of sample (A), 3D rendering (B), septate fiber (arrowhead) (C), transverse section shows axial parenchyma band (a) and vessel grouping of solitary (s) and radial multiple (rm) (D), radial section shows heterogenous ray cells (E), prismatic crystal (arrowhead) in axial parenchyma (F).

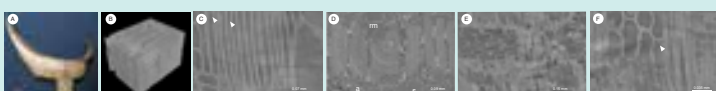


**Figure 2.** Observation of sample WR-002: photograph of sample (A), 3D rendering (B), septate fiber (arrowhead) (C), transverse section shows axial parenchyma band (a) and vessel grouping of solitary (s) and radial multiple (rm) (D), radial section shows homogenous ray cells (E), deposit (arrowhead) in axial parenchyma (F).

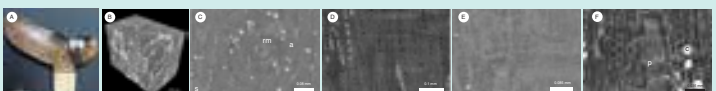


**Figure 3.** Observation of sample WR-003: photograph of sample (A), 3D rendering (B), transverse section shows axial parenchyma band (a) and vessel grouping of solitary (s) and radial multiple (rm) (C), tangential section shows uniseriate ray (D), radial section shows heterogenous ray cells (E), prismatic crystal in axial parenchyma (c) and simple perforation plate (p) (F).

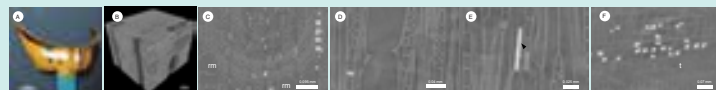


**Figure 4.** Observation of sample WR-004: photograph of sample (A), 3D rendering (B), transverse section shows vessel grouping of radial multiple (rm) (C), tangential section shows simple perforation plate (D), needle-shaped crystal (arrowhead) (E), radial section shows tile cells (t) and prismatic crystal in ray parenchyma (c) (F).

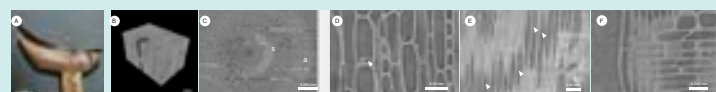


**Figure 5.** Observation of sample WR-005: photograph of sample (A), 3D rendering (B), transverse section shows vessel grouping of solitary (s) (C), deposit in axial parenchyma (arrowhead) (D), septate fiber (arrowhead) (E), radial section shows heterogeneous ray cells (F).

### Flatten vessel element surface

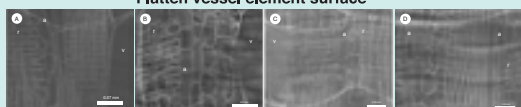


**Figure 6.** Flatten vessel element surface: sample WR-001 (A), sample WR-002 (B), sample WR-004 (C), sample WR-005 (D). r: vessel-ray pit, a: vessel-axial parenchyma pit, v: intervessel pit

### Prismatic crystal arrangement

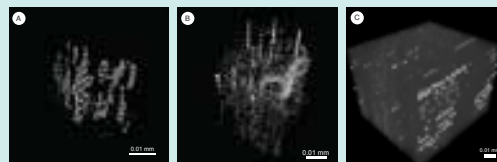


**Figure 7.** Prismatic crystal arrangement: sample WR-001 (A), sample WR-003 (B), sample WR-004 (C).

**Table 1. Summary of samples anatomical features**

Anatomical features	WR-001	WR-002	WR-003	WR-004	WR-005
Vessel grouping	solitaire, radial multiple 2	solitaire, radial multiple 2	solitaire, radial multiple 3	radial multiple 2-3	solitaire
Vessel length	400-470 µm	270-340 µm	140-280 µm	240-290 µm	330-390 µm
Diameter of vessel lumen	70-80 µm	80-90 µm	60-80 µm	80-90 µm	90-100 µm
Perforation plate	simple	simple	simple	simple	simple
Intervessel pit	alternating, closed	alternating, closed	-	alternating, less crowded	-
Vessel-ray pit	horizontal, growing, less crowded	horizontal, growing, less crowded	-	horizontal, growing, less crowded	horizontal, growing, less crowded
Vessel-axial parenchyma	longitudinal series, closed	longitudinal series, closed	-	longitudinal series, less crowded	longitudinal series, closed
Septate fiber	present	present	-	present	present
Ray cellular composition	heterogeneous	heterogeneous	heterogeneous	heterogeneous	heterogeneous
Ray width	1-2 series	1-3 series	1-3 series	1-3 series	1-3 series
Crystal	axial parenchyma	-	axial parenchyma	axial parenchyma	-
axial parenchyma type	altern. band	band more than 3 cells wide	confluent	diffuse in square	narrow band (up to 3 cells wide)
Tile cells	-	-	-	present	-

### Identification Result

WR-001	WR-002	WR-003	WR-004	WR-005
This transverse section of this sample almost identical with WR-002, the main differences are abundance of prismatic crystal on WR-001 (Fig. 7A), and different pattern of contact area on observed vessel element (Fig. 6A and 6B).	This sample has solitary and radial multiple vessel (Fig. 2D), axial parenchyma band more than 3 cells wide (Fig. 2D), and septate fibers (Fig. 2C) which is probably <i>Dysoxylum</i> sp.	This sample has axial parenchyma confluent (Fig. 3C), heterogeneous ray cells (Fig. 3E), three cells per parenchyma strand (Fig. 3B) which is probably <i>Mangifera</i> sp.	This sample has axial parenchyma diffus-in-aggregate (Fig. 4C), prismatic crystal in ray parenchyma cells (Fig. 4F) and the cells (Fig. 4E) which is similar to <i>Kleinhovia hospita</i> .	This sample has solitary vessel (Fig. 5C), axial parenchyma narrow (up to 3 cells wide) band (Fig. 5C), and abundant septate fibers (Fig. 5E) which is probably <i>Dysoxylum</i> sp.

## Acknowledgement

The synchrotron radiation experiments were performed at SPring-8 with the approval of the Japan Synchrotron Radiation Research Institute (Proposal No. 2016B1743). The authors thanks to Dr. Fajar Waskito and Mr. Taufiq Hermawan for providing wooden sheath samples